European Journal of Radiology 205 (2026) 113193

Contents lists available at ScienceDirect

European Journal of Radiology

journal homepage: www.elsevier.com/locate/ejrad

Where no sound wave has gone before: first high-resolution transcranial images of the brain using ultrasound computed tomography

Thomas J. Marini [*,1], Trevor Mitcham [1], Rehman Ali, Israel Owolabi, Victoria Nketia, Matthew T. Bender, Gurkirat Kohli, Santiago Mendoza-Ayus, Marissa Lake, Melanie Singh, Alex Klaben, Mohammad Mehrmohammadi, Timothy M. Baran, Deborah Rubens, James Bai, Shehanaz Ellika, Alexander Kessler, Anthony Portanova, Stephen M. Smith, Adam Dykie, Yu T. Zhao, Hossein Raeis, Gaofei Jin, David Bustamante, Eric Miller, Josephine Buffum, Nebojsa Duric

University of Rochester Medical Center, 601 Elmwood Avenue, Rochester, NY 14642, USA

ARTICLE INFO

Keywords:
Ultrasound
Ultrasound tomography
Brain
Hemorrhage
Stroke
Point-of-care imaging

ABSTRACT

Background: Point-of-care imaging of the brain is a major unmet need. Attenuation of ultrasound by the skull hinders sonographic evaluation of the brain in adults.
Purpose: Ultrasound tomography holds potential in sonographic imaging of the brain through the skull. This work assesses the ability of a commercial ultrasound tomography machine to image the human brain.
Materials and Methods: A cadaveric specimen was prospectively imaged in the SoftVue commercial ultrasound tomography machine from August to September 2025. A neurosurgeon placed a 40-cc water-filled inclusion in the left cerebral hemisphere intended to mimic hemorrhage. Ultrasound tomography was obtained before and after the inclusion placement without and with an intervening cadaver skull. Fellowship trained neuroradiologists assessed the images for quality and visualization of key anatomic structures and inclusions. Sound speed values, signal-to-noise ratios, and contrast-to-noise ratios were also calculated on the acquired images.
Results: Ultrasound tomography allowed visualization of basic brain anatomy without a skull. The spatial resolution of the images without the skull was approximately 0.75 mm. Additionally, the implanted water-filled inclusion mimicking hemorrhage was visualized through the skull per neuroradiologist assessment. The implanted inclusion could also be quantitatively identified as different from the surrounding normal anatomy.
Conclusion: Ultrasound tomography allowed visualization of major brain anatomy and a water-filled inclusion mimicking hemorrhage in the brain parenchyma demonstrating potential utility in neuroimaging. Ultrasound tomographic images through the skull visualizing the water-filled inclusion mimicking hemorrhage were also obtained showing the potential value of ultrasound tomography in intact samples.

1. Introduction

Neurological disease states including stroke, traumatic brain injury, tumors, and autoimmune disease have widespread impact on population health and healthcare systems [1–4]. Stroke, in particular, is the second highest cause of disability and death worldwide with over 10 million strokes estimated per year [5]. Intracranial hemorrhage results in an estimated 3 million deaths globally per year with significant morbidity [6,7]. Neuroimaging plays an invaluable role in the diagnosis and management of these conditions [8]. While neuroimaging is vital in timely and accurate diagnosis, point-of-care imaging of the brain has traditionally been limited in use due to the nature and constraints of CT and MRI imaging. These are expensive to purchase and maintain, minimally portable, and require highly trained operators [9,10]. Therefore, widespread point-of-care imaging for the brain has been elusive. This lack of point-of-care imaging is to the detriment of patient

Abbreviations: UST, Ultrasound tomography; CNR, Contrast-to-noise ratio; FWI, Full-waveform inversion; ROI, Region of interest; SNR, Signal-to-noise ratio.

* Corresponding author.
E-mail address: Rochesterradiology2021@gmail.com (T.J. Marini).
[1] Co-first authors.

https://doi.org/10.1016/j.ejrad.2026.113193
Received 9 April 2026; Received in revised form 25 June 2026; Accepted 25 August 2026
Available online 27 August 2026

care as clinicians often cannot optimally manage patients without imaging of the brain potentially delaying care and increasing morbidity/mortality. While ultrasound is readily amenable to imaging of the brain parenchyma itself, the skull has traditionally limited evaluation of the brain due to its strong attenuation and aberration of sound waves. Ultrasound tomography (UST) of the brain has the potential to fill this gap and make a substantial difference in patient care allowing rapid radiation-free ultrasound imaging at the point-of-care through the skull.

UST is a relatively new imaging modality that has shown recent success in utilization for breast cancer screening [11]. Unlike traditional ultrasound modalities, UST utilizes a closed-geometry ring transducer that analyzes both reflected and transmitted ultrasound signals. Due to this unique setup, UST can be used to generate quantitative estimates of tissue properties such as sound speed, density, and acoustic attenuation using a novel full-waveform inversion (FWI) reconstruction technique [12]. These image reconstructions allow for quantitative image results, similar to those from classic CT imaging, which can be used to clearly distinguish abnormal tissue properties. However, UST is also capable of providing a classical delay-and-sum reflection image in addition to these quantitative tissue maps, which allows for multiple views of a given image slice to aid in diagnosis. While UST has received FDA approval for adjunctive breast cancer screening, imaging the brain through the skull provides a new set of challenges which must be addressed.

The largest barriers to the development of UST for use in the brain are attenuation/aberration of ultrasound by the skull and large refractions at the skull-brain interface [13]. Despite these obstacles, preliminary evidence has suggested the promise of UST for imaging of the brain [13–16]. UST benefits from the use of ultra-low ultrasound frequencies (i.e., ultrasonic frequencies below 1 MHz) which can penetrate the skull better than traditional clinical frequencies, while maintaining high (sub-mm) spatial resolution. An UST system capable of transcranial imaging could potentially bring neuroimaging to patients at the point-of-injury including in ambulances, clinics, hospitals, and austere settings (including military field hospitals). An all-ultrasound neuroimaging device would be relatively low-cost (both to purchase and maintain), rapid, produce no ionizing radiation, and utilize no contrast agents. Early identification and treatment of both stroke and hemorrhage is critical to ensure lowest morbidity and mortality [17,18]. With further technical development and refinement, UST could be deployed to allow earlier detection of both ischemia and hemorrhage, expediting treatment. In low- and middle-income countries, brain UST could potentially allow sustainable imaging in areas without CT scanners or MRI [19,20].

We hypothesized that a commercial UST machine originally designed for breast imaging could demonstrate feasibility for imaging the brain in a cadaveric model. In this study, we sought to assess the image quality of UST in a cadaveric specimen with the goal of demonstrating the potential of UST to image brain parenchyma.

Methods

This study utilized a Philips Ingenuity 128 CT system (Amsterdam, Netherlands) and a SoftVue UST system produced by Delphinus Medical Technologies (Novi, Michigan) for data collection. The CT scanner operated at a kVp of 120 and a mAs of 337 for the intact head and a kVp of 100 and a mAs of 337 for the dissected brain to generate baseline images for comparison. The SoftVue system used a 512-channel data acquisition system with a 2:1 multiplexer connected to a 1024-element ring array (3 MHz center frequency, 1-4 MHz 6-dB bandwidth) (Figs. 1 and 2). A broadband pulse centered at 2.5 MHz was applied to the

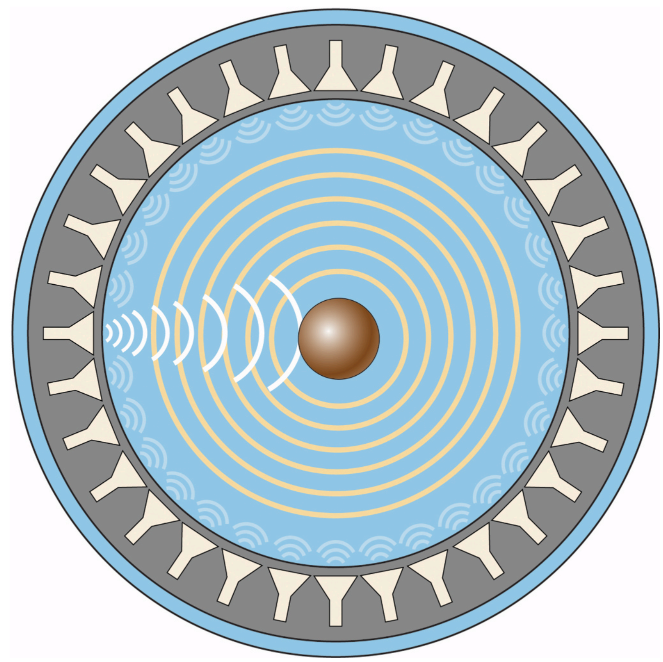

Fig. 2. Schematic of Ultrasound Tomography. Illustration showing conceptually how ultrasound tomography functions. Each element in the ring transducer emits a signal which is received by all the other elements in the ring. This pattern repeats itself until each element has emitted a signal.

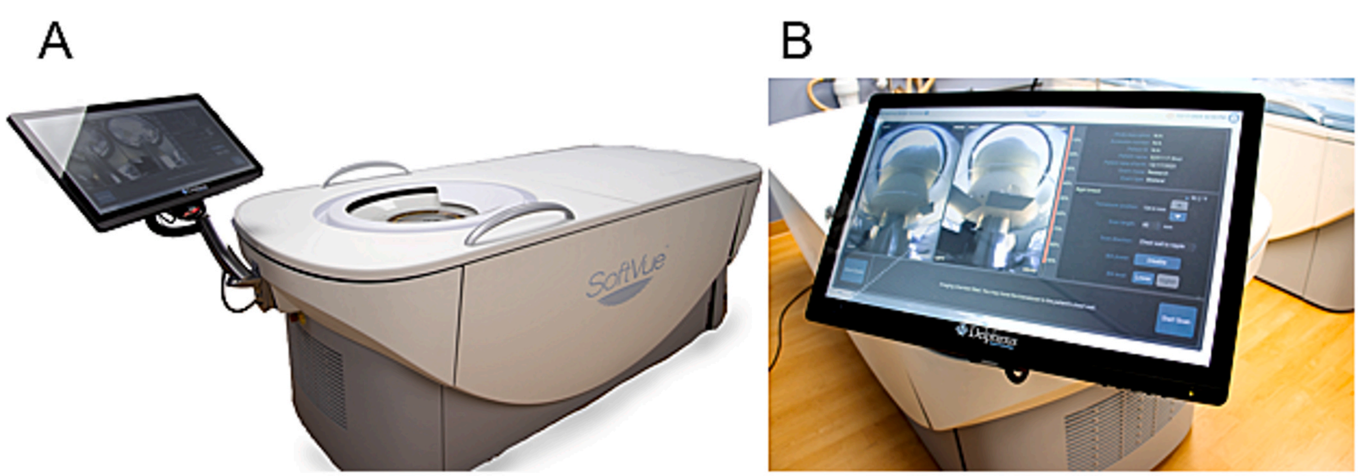

Fig. 1. SoftVue Commercial Ultrasound Tomography Machine. (A) Photo of the SoftVue ultrasound tomography machine used to obtain images in this study. (B) Photo of the screen used to set machine settings with video of the water bath.

transducer to generate data between 150 kHz and 4 MHz (detectable signals above the noise floor). Although the bulk of the frequency content is between 1-4 MHz, the SoftVue setup preserves the low-frequency signal content to enable both reflection and transmission imaging (Supplemental Fig. 1). Raw radiofrequency data were acquired using an approach in which one element is excited at a time, while all other elements receive the signal from that element. This cycle was repeated until data from the full rotation of the transmit signals around the ring had been collected. The system then moved the ring transducer in successive 2.5 mm steps in the craniocaudal direction, until the full dataset had been acquired (Supplemental Video 1).

Image reconstruction was performed using a frequency-domain FWI algorithm [12,14,21,22]. To briefly describe how FWI works, a 2D numerical model of the Helmholtz equation is used to simulate the expected signal generated by the system with a homogeneous starting model [12]. The result of this simulation is then iteratively compared to the measured data at each discrete frequency, starting at the lowest available frequency and subsequently increasing to the highest desired frequency value with set spacing. The error between the forward model and acquired data is then backprojected to update the sound speed profile at each iteration until the error is minimized. Despite its robustness, FWI is susceptible to cycle skipping artifacts if the simulated signal is more than half a wavelength out of phase from the experimental data. As low frequencies result in longer wavelengths, the most straightforward method to reduce cycle skipping artifacts is to lower the initial frequency used for reconstruction.

The ultrasound data are reconstructed to provide distinct imaging sequences of sound speed (related to tissue density) and reflection (related to anatomic information) for radiologist review. For all images of the brain by itself, sound speed images were reconstructed using FWI reconstruction with the standard clinical SoftVue FWI algorithm. The reconstruction was performed from 300 kHz to 1 MHz with 50 kHz step sizes [14]. For images of the brain inside the human skull, sound speed images were reconstructed using an offline MATLAB implementation of FWI, using data from 150-700 kHz with 50 kHz step size and a 1550 m/s homogeneous starting model. Finally, all reflection images are generated using delay-and-sum beamforming, where a localized subset of receiving elements around each transmitting element was used for beamforming. Individual sub-aperture images were reconstructed for each transmit position, and then compounded around the full ring to form the final image. The sound speed map resulting from FWI was incorporated into the beamforming step to correct for aberrations induced by heterogeneity in sound speed within the image space.

For all experimental testing, a cadaveric specimen was purchased through the company Science Care (Aurora, Colorado). Science Care is accredited by the Association for Advancing Tissue and Biologics and follows strict ethical guidelines regarding cadavers. In addition, all our own institutional guidelines for use of cadaver specimens were followed including treating specimens with the utmost dignity and ensuring safeguards against public viewing. The specimen was preserved in a combination of formaldehyde and methanol for approximately 2 months prior to imaging. A neurosurgeon first performed a craniotomy removing the brain from the skull. The unmanipulated brain was then imaged with UST both with and without the cadaveric skull present, providing reference imaging prior to surgical manipulation. Imaging on SoftVue was performed by placing the cadaveric specimen in distilled water-filled bags (Fig. 3a). The bag was then placed in the 37°C water bath at physiologic body temperature for imaging. Following this initial imaging, a neurosurgeon placed a 40-cc water-filled condom in the left centrum semiovale/corona radiata anteriorly meant to simulate a parenchymal brain hemorrhage. Water was chosen for this initial experiment as it was expected to provide sufficient sound speed contrast with the preserved brain to appropriately mimic a hemorrhage in a healthy brain. Specifically, the difference between water (1515 m/s) and the preserved tissue (~1600 m/s) is in the same range as that of healthy brain tissue (1540 m/s) and blood (1580-1630 m/s) [23,24]. The manipulated brain with a single inclusion was then imaged by itself and then with the cadaveric skull surrounding it in the UST system (Fig. 3b). UST imaging was performed with standard machine settings as described above with a video of an acquisition seen in Supplemental Video 1. CT scans were performed of the initial intact specimen, the dissected brain after craniotomy, and the brain after the first inclusion placement.

To assess the clinical utility of the UST images, 5 diagnostic fellowship-trained neuroradiologists reviewed the acquired UST dataset, initially without the skull evaluating basic neuroanatomy on a consensus basis. Subsequently, the imaging with a skull was reviewed to assess for the water-filled inclusion. The UST images were assessed in relation to CT imaging as a ground truth. Finally, the imaging features in the sound speed images in Figs. 5 and 6 were assessed by generating three 6-mm diameter circular regions of interest (ROIs) within brain and the inclusion (Fig. 5C). Sound speed values in each region are reported as the mean value across all three ROIs with the standard deviation between ROIs reported as the error. Additionally, each ROI was expanded to create an annulus of equal areas fully surrounding each ROI with the same centroid. Information from the circular ROI and secondary annulus

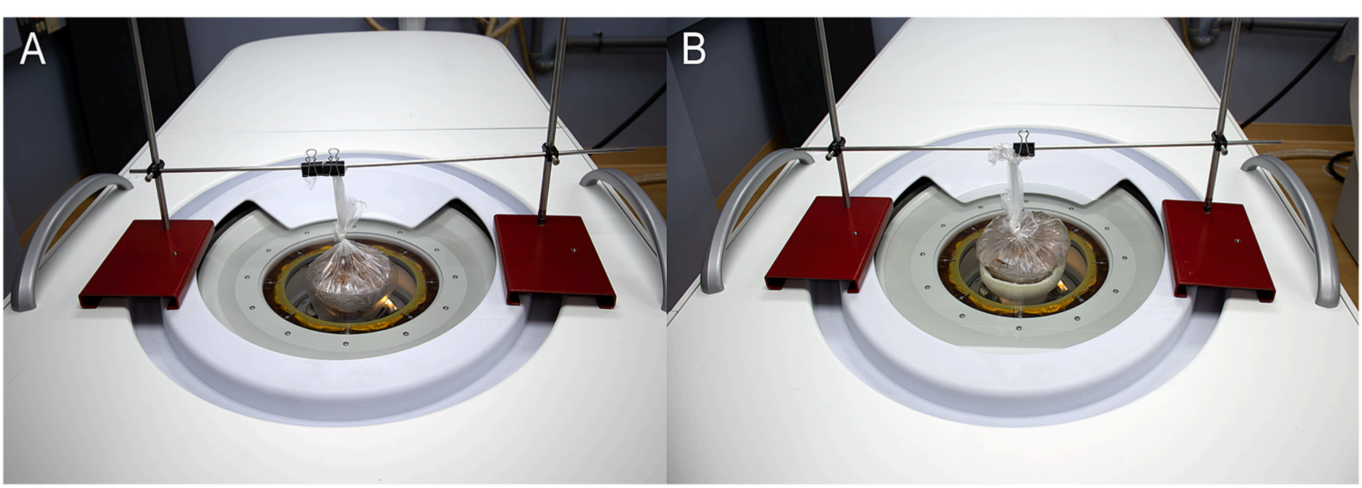

Fig. 3. Experimental Setup. (A) Photo showing the imaging setup for a cadaveric brain without a skull. The brain is immersed in distilled water in a transparent plastic bag and secured to an overlying bar with clips. The bagged brain is placed in the center of the water bath for imaging. (B) Photo showing the imaging setup for a cadaveric brain in a degassed cadaveric skull. The brain is again placed in a plastic bag secured to an overlying bar. The brain is subsequently placed inside the degassed cadaveric skull for imaging in the water bath.

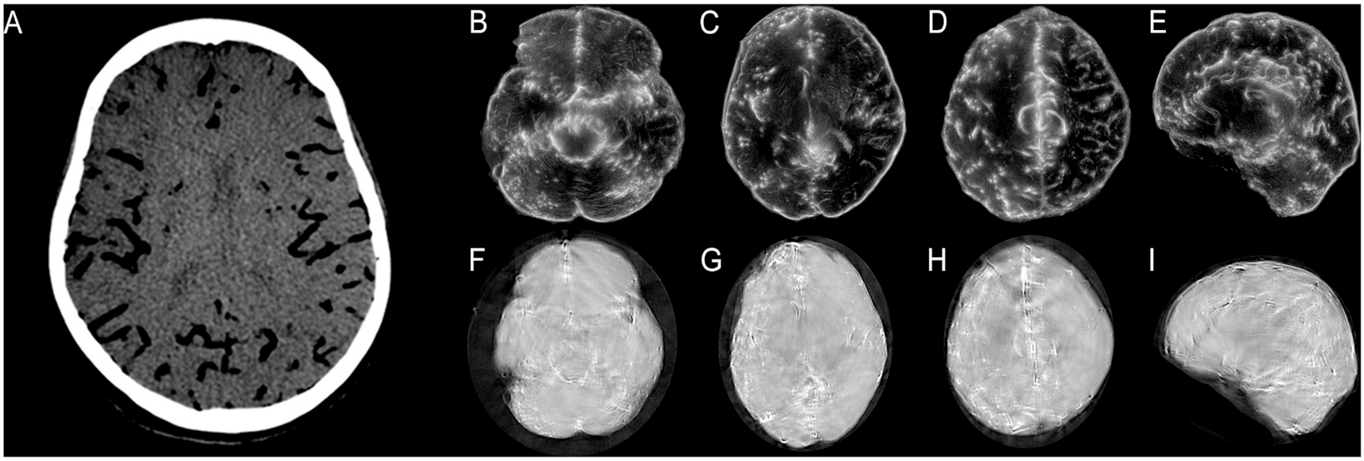

Fig. 4. SoftVue Ultrasound Tomographic Imaging of a Brain Without a Skull. (A) Axial CT image of the cadaver brain through the level of the lateral ventricles. Axial reflection ultrasound tomographic imaging of the brain at the level of the midbrain (B), lateral ventricles/corona radiata (C), and centrum semiovale (D). (E) Sagittal reflection ultrasound tomographic image of the brain through the corpus callosum. Both axial and sagittal reflection imaging demonstrates key brain landmarks including sulci, gyri, interhemispheric fissure, choroid plexus, cerebellum, and brainstem. (F, G, H, I) Corresponding sound speed images to the reflection images.

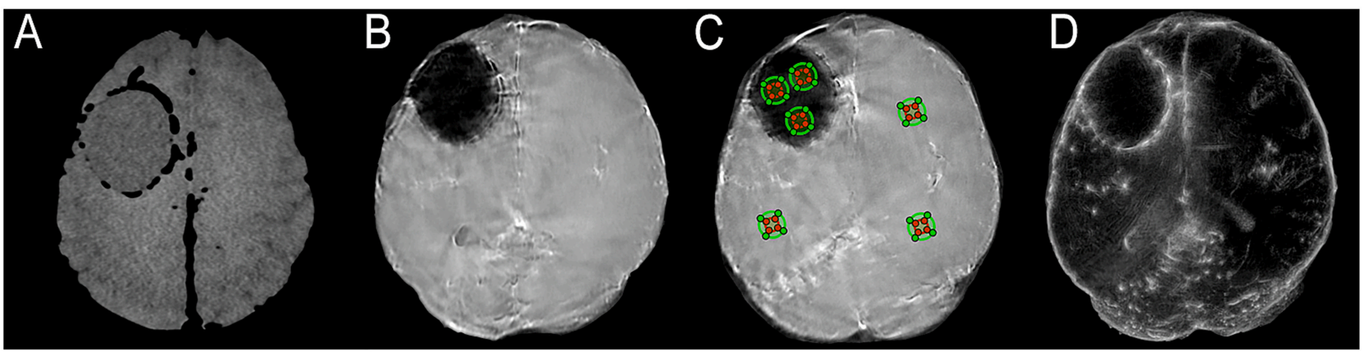

Fig. 5. SoftVue Ultrasound Tomographic Imaging of a Brain with a Water-Filled Inclusion Mimicking Hemorrhage Without a Skull. (A) Axial CT image of a 40-cc water-filled inclusion mimicking hemorrhage placed in the left centrum semiovale anteriorly. (B) Axial sound speed ultrasound tomographic image of the brain showing the inclusion in the left centrum semiovale anteriorly. On sound speed imaging, the water-filled inclusion appears dark relative to the brain parenchyma. (C) Sound speed image demonstrating region of interest placement. (D) Axial reflection ultrasound tomographic image of the brain showing the inclusion in the left centrum semiovale anteriorly. On reflection imaging, the water-filled inclusion again appears dark relative to the brain parenchyma.

ROI were used to calculate signal-to-noise ratio (SNR) and contrast-to-noise ratio (CNR) as follows:

$$SNR = 20*log_{10}\frac{s_i}{\sigma_o} \quad (1)$$

$$CNR = \frac{s_i - s_o}{\sqrt{\sigma_i^2 + \sigma_o^2}} \quad (2)$$

Where s_i is the signal inside the circular ROI, s_o is the signal in the surrounding annulus, σ_i is the standard deviation within the circular ROI, and σ_o is the standard deviation of the surrounding annulus.

2. Results

All neuroradiologists reported clear visualization of anatomical brain structures on SoftVue imaging of the brain without a skull. Reflection imaging provided the highest level of anatomic detail (Fig. 4). Major neuroanatomical landmarks on both UST and CT were identified including the cerebral hemispheres, interhemispheric fissure, corpus callosum, cerebellum, brainstem, and choroid plexus. The water-filled inclusion meant to mimic a hemorrhage was easily recognized on sound speed imaging by all radiologists (Fig. 5). Radiologists also confirmed visualization of the inclusion on the reconstructed images through the skull (Fig. 6 and Supplemental Video 2). Brain anatomy was unable to be delineated on the UST imaging through the skull.

The spatial resolution of the images without the skull was approximately 0.75 mm, which is consistent with the theoretical resolution of UST of $\lambda/2$, where λ is the wavelength of the highest reconstructed frequency (in this case 1 MHz). The spatial resolution of images obtained through the skull was approximately 1 mm, due to the reconstruction finishing at 700 kHz. Although this resolution is worse than the other images, it is nonetheless sufficient to visualize the simulated hemorrhage through the skull.

The sound speed values of regular brain tissue were 1599 m/s ± 1.6 in the brain by itself, and 1584 m/s ± 4.3 in the brain within the skull. The sound speed values of the water-filled inclusion were 1508 m/s ± 2.3 in the brain by itself, and 1532 m/s ± 1.0 in the brain within the skull. SNR values without the presence of the skull were 49.4 dB ± 2.3 and 48.1 ± 2.6, respectively for regular brain tissue and the inclusion. With the skull present, they remained similar at 46.4 dB ± 1.7 and 44.6 dB ± 1.3, respectively. CNR values followed the same trend, with values of 0.347 ± 0.15, 0.271 ± 0.05, 0.377 ± 0.04, and 0.469 ± 0.10 for regular brain and the inclusion without and with the skull, respectively.

3. Discussion

In this study, we have provided evidence of the potential of SoftVue UST to image brain parenchyma without and with a skull. To our

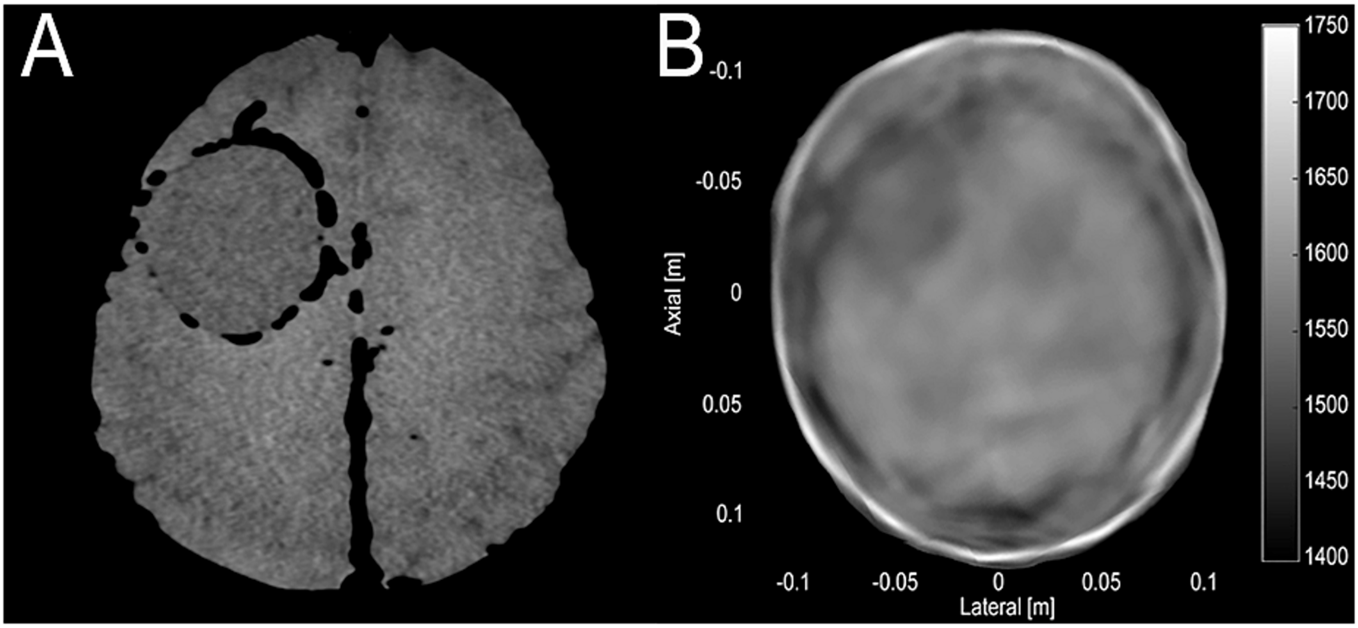

Fig. 6. SoftVue Ultrasound Tomographic Imaging of a Brain with a Water-Filled Inclusion Mimicking Hemorrhage Through a Cadaveric Skull. (A) Reference axial CT imaging showing the 40-cc water-filled inclusion mimicking hemorrhage in the left centrum semiovale anteriorly. (B) Axial sound speed ultrasound tomographic image of the brain through the skull showing the inclusion in the left centrum semiovale anteriorly. The water-filled inclusion appears dark relative to the background brain parenchyma.

knowledge, we are reporting the first results from UST imaging of the brain through the skull using FWI reconstruction. The UST imaging without a skull allowed assessment of major brain anatomy with complete agreement and confidence among radiology readers. Similarly, a water-filled hemorrhage-mimicking inclusion was readily identified by neuroradiologists on these images both with and without the skull. While diagnostic assessment of anatomy is not possible through the skull at this time, results show the potential of UST to image pathology through the skull even in this early stage of technical development. A rudimentary UST system capable of detecting brain hemorrhage could better improve management of brain bleeds and strokes in a variety of settings irrespective of the ability to delineate detailed anatomy.

Limitations of this study are partially rooted in the non-optimal frequencies used by the commercial system. The SoftVue system is optimized for breast imaging with a central frequency of 3 MHz. Thus, the ultra-low frequency signals (i.e., <1 MHz) needed to penetrate the skull have relatively poor SNR. While the tomographic compounding still makes good use of the available signal and generates quality images of the brain, image degradation is severe when imaging through the skull. Although this limits the assessment of detailed brain anatomy, the water-filled inclusion mimicking hemorrhage was still visualized showing the ability to obtain meaningful diagnostic information. A future commercial UST system optimized for imaging of the brain would optimize signal SNR in the 100-800 kHz range. This would lead to significant image quality improvement and additional potential to image a variety of disease states including intracranial hemorrhage. Such a system would also be developed to account for the unique curvature of the human skull, which the current breast cancer screening system cannot do. Coupling the transducer elements to the scalp will also be a unique challenge, requiring either dry coupling or a thin water layer within the helmet to ensure acoustic coupling. Although hair does not provide significant attenuation at the frequencies used in this work, it will be important to ensure that the patient's hair does not trap air inside during the coupling as well. Additionally, using classical FWI reconstruction with a homogeneous starting model may not be sufficient to provide diagnostic quality images through the skull; further areas of algorithmic investigation include optimized starting models and advanced reconstruction techniques to ensure high fidelity imaging through the skull [25–28]. It should also be noted that the preservation of the cadaver in formaldehyde and methanol alters tissue properties from those seen in live human subjects. Future testing can continue to incorporate cadaver models for convenience and safety, but the limitations of preserved cadaver specimens should be carefully considered in both the design and interpretation of experiments.

The development and testing of UST with this goal of a new high-quality method for point-of-care brain imaging has the potential to usher a paradigm shift in neurological care. The majority of the global population is thought to lack access to any form of medical imaging. This work highlights UST's appeal for use in a global health context especially in rural areas and military hospitals [29]. UST could also help lower radiation exposure and allow more frequent examination for lower-cost and closer follow-up. There would also be potential use in clinics to screen for intracranial hemorrhage or tumors in patients with headache. Since UST can assess tissue stiffness it could have other uses in neuro-oncology and neurodegenerative disease. Ultimately, the potential applications of UST could be quite broad, but further proof of concept work is needed to guide the development of a clinical system prototype.

In this study we have shown the potential of UST to image the brain both without and with a skull. Without a skull, UST was able to image the brain with sufficient quality to identify normal brain anatomy including the cerebral hemispheres, ventricular system, brainstem, and cerebellum. With the introduction of a skull, imaging was limited to allowing visualization of the water-filled inclusion mimicking hemorrhage. Future studies should attempt to optimize UST for imaging of the brain including by utilizing lower frequency transducers, optimizing transducer geometries to account for the unique shape of the skull, and developing better reconstruction algorithms. These studies can also seek to assess the effect of differences in skull thickness and inclusion sizes. Given the groundwork conducted in this study, such work could ultimately lead to a rapid, portable, cost-effective, sonographic imaging system for point-of-care assessment of the brain.

CRediT authorship contribution statement

Thomas J. Marini: Writing – review & editing, Writing – original draft, Visualization, Validation, Supervision, Resources, Project administration, Methodology, Investigation, Funding acquisition, Formal analysis, Data curation, Conceptualization. **Trevor Mitcham:** Writing – review & editing, Writing – original draft, Visualization, Validation, Supervision, Resources, Project administration, Methodology, Investigation, Funding acquisition, Formal analysis, Data curation, Conceptualization. **Rehman Ali:** Writing – review & editing, Validation, Supervision, Resources, Project administration, Methodology, Investigation, Formal analysis, Data curation, Conceptualization. **Israel Owolabi:** Writing – review & editing, Methodology, Investigation, Data curation. **Victoria Nketia:** Writing – review & editing, Methodology, Investigation, Data curation. **Matthew Bender:** Writing – review & editing, Supervision, Resources, Project administration, Methodology, Investigation, Funding acquisition, Conceptualization. **Gurkirat Kohli:** Writing – review & editing, Methodology, Investigation. **Santiago Mendoza Ayus:** Writing – review & editing, Methodology, Investigation. **Marissa Lake:** Writing – review & editing, Resources, Project administration. **Melanie Singh:** Writing – review & editing, Investigation, Conceptualization. **Alexander Klaben:** Writing – review & editing, Investigation, Conceptualization. **Mohammad Mehrmohammadi:** Writing – review & editing, Resources, Project administration, Methodology, Investigation, Conceptualization. **Timothy M. Baran:** Writing – review & editing, Writing – original draft, Resources, Investigation, Funding acquisition, Data curation, Conceptualization. **Deborah Rubens:** Writing – review & editing, Project administration, Methodology, Investigation, Funding acquisition, Conceptualization. **James Bai:** Writing – review & editing, Investigation, Formal analysis. **Shehanaz Ellika:** Writing – review & editing, Investigation, Formal analysis. **Alexander Kessler:** Writing – review & editing, Methodology, Formal analysis. **Anthony Portanova:** Writing – review & editing, Formal analysis, Conceptualization. **Stephen M. Smith:** Writing – review & editing, Investigation, Formal analysis. **Adam Dykie:** Writing – review & editing, Investigation. **Yu Zhao:** Writing – review & editing, Investigation. **Hossein Raeis:** Writing – review & editing, Investigation, Conceptualization. **Gaofei Jin:** Writing – review & editing, Investigation, Conceptualization. **David Bustamante:** Writing – review & editing, Investigation, Conceptualization. **Eric Miller:** Writing – original draft, Resources, Investigation. **Josephine Buffum:** Writing – review & editing, Resources, Investigation. **Nebojsa Duric:** Writing – review & editing, Writing – original draft, Visualization, Validation, Supervision, Resources, Project administration, Methodology, Investigation, Funding acquisition, Formal analysis, Data curation, Conceptualization.

Declaration of competing interest

The authors declare that they have no known competing financial interests or personal relationships that could have appeared to influence the work reported in this paper.

Acknowledgements

This work was funded by the Radiological Society of North America through a Research Scholar Grant. We thank Sarah Klingenberger, Jane Lichoworic, and Gwen Mack for their help with the illustrations and figures. We thank Karen Klindt and Carol Young for administrative assistance.

Appendix A. Supplementary data

Supplementary data to this article can be found online at https://doi.org/10.1016/j.ejrad.2026.113193.

References:

[1] A.A. Hyder, C.A. Wunderlich, P. Puvanachandra, G. Gururaj, O.C. Kobusingye, The impact of traumatic brain injuries: a global perspective, NeuroRehabilitation 22 (5) (2007) 341–353.
[2] J.A. Langlois, W. Rutland-Brown, M.M. Wald, The epidemiology and impact of traumatic brain injury: a brief overview, The Journal of head trauma rehabilitation 21 (5) (2006) 375–378.
[3] C.D. Wolfe, The impact of stroke, British medical bulletin 56 (2) (2000) 275–286.
[4] C.W. Tsao, A.W. Aday, Z.I. Almarzooq, C.A.M. Anderson, P. Arora, C.L. Avery, C. M. Baker-Smith, A.Z. Beaton, A.K. Boehme, A.E. Buxton, Y. Commodore-Mensah, M.S.V. Elkind, K.R. Evenson, C. Eze-Nliam, S. Fugar, G. Generoso, D.G. Heard, S. Hiremath, J.E. Ho, R. Kalani, D.S. Kazi, D. Ko, D.A. Levine, J. Liu, J. Ma, J. W. Magnani, E.D. Michos, M.E. Mussolino, S.D. Navaneethan, N.I. Parikh, R. Poudel, M. Rezk-Hanna, G.A. Roth, N.S. Shah, M.P. St-Onge, E.L. Thacker, S. S. Virani, J.H. Voeks, N.Y. Wang, N.D. Wong, S.S. Wong, K. Yaffe, S.S. Martin, Heart Disease and Stroke Statistics-2023 Update: A Report From the American Heart Association, Circulation 147 (8) (2023) e93–e621.
[5] V. Saini, L. Guada, D.R. Yavagal, Global Epidemiology of Stroke and Access to Acute Ischemic Stroke Interventions, Neurology 97 (20 Suppl 2) (2021) S6–s16.
[6] T. Sun, Y. Yuan, K. Wu, Y. Zhou, C. You, J. Guan, Trends and patterns in the global burden of intracerebral hemorrhage: a comprehensive analysis from 1990 to 2019, Frontiers in neurology 14 (2023).
[7] L. Xu, Z. Wang, W. Wu, M. Li, Q. Li, Global, regional, and national burden of intracerebral hemorrhage and its attributable risk factors from 1990 to 2021: results from the 2021 Global Burden of Disease Study, BMC Public Health 24 (1) (2024) 2426.
[8] T.A. Milligan, Diagnosis in Neurologic Disease, Medical Clinics of North America 103 (2) (2019) 173–190.
[9] P. Hariharan, M.B. Tariq, J.C. Grotta, A.L. Czap, Mobile Stroke Units: Current Evidence and Impact, Curr Neurol Neurosci Rep 22 (1) (2022) 71–81.
[10] A. Shoghli, D. Chow, E. Kuoy, V. Yaghmai, Current role of portable MRI in diagnosis of acute neurological conditions, Frontiers in neurology 14 (2023) 1255858.
[11] P.J. Littrup, M. Mehrmohammadi, N. Duric, Breast Tomographic Ultrasound: The Spectrum from Current Dense Breast Cancer Screenings to Future Theranostic Treatments, Tomography 10 (4) (2024) 554–573.
[12] R. Ali, G. Jin, M. Singh, T. Mitcham, N. Duric, 3D Frequency-Domain Full Waveform Inversion for Whole-Breast Imaging With a Multi-Row Ring Array, IEEE Open J Ultrason Ferroelectr Freq Control 5 (2025) 77–81.
[13] T. Mitcham, R. Ali, M. Singh, S. McConnell, R. Rahmani, D. Schartz, M. Bender, E. Vates, N. Duric, Transcranial ultrasound tomography for brain imaging: Ex vivo results and potential for stroke imaging, Medical physics 52 (10) (2025) e18090.
[14] R. Ali, T. Mitcham, N. Duric, Impact of starting model on waveform inversion in ultrasound tomography, Proc. SPIE 12470, Medical Imaging 2023: Ultrasonic Imaging and Tomography 52 (10 Apr 2023) 124700J, https://doi.org/10.1117/12.2653575.
[15] R. Ali, T. Mitcham, M. Singh, et al., Distributed aberration correction in handheld ultrasound based on tomographic estimates of the speed of sound, Proc. SPIE 12470, Medical Imaging 2023: Ultrasonic Imaging and Tomography (10 Apr 2023) 1247009, https://doi.org/10.1117/12.2653935.
[16] T. Mitcham, R. Ali, D. Schartz, M. Singh, M. Bender, N. Duric, Feasibility of Imaging Ischemic Stroke Through the Skull Using Ultrasound Tomography, IEEE International Ultrasonics Symposium (IUS) 2023 (2023) 1–3.
[17] J.L. Saver, Time is brain–quantified, Stroke 37 (1) (2006) 263–266.
[18] K.N. Sheth, N. Solomon, B. Alhanti, S.R. Messe, Y. Xian, D.L. Bhatt, J.C. Hemphill, J.A. Frontera, R.C. Chang, I.M. Danelich, J. Huang, L. Schwamm, E.E. Smith, J. N. Goldstein, B. Mac Grory, G.C. Fonarow, J.L. Saver, Time to Anticoagulation Reversal and Outcomes After Intracerebral Hemorrhage, JAMA Neurology 81 (4) (2024) 363–372.
[19] D.S. Maru, R. Schwarz, A. Jason, S. Basu, A. Sharma, C. Moore, Turning a blind eye: the mobilization of radiology services in resource-poor regions, Global Health 6 (2010) 18.
[20] P.S. Ngoya, W.E. Muhogora, R.D. Pitcher, Defining the diagnostic divide: an analysis of registered radiological equipment resources in a low-income African country, Pan Afr Med J 25 (2016) 99.
[21] F. Li, U. Villa, N. Duric, et al., 3D full-waveform inversion in ultrasound computed tomography employing a ring-array", Proc. SPIE 12470, Medical Imaging 2023: Ultrasonic Imaging and Tomography, Proc. SPIE 12470, Medical Imaging 2023: Ultrasonic Imaging and Tomography (10 Apr 2023) 124700K, https://doi.org/10.1117/12.2654406.
[22] F. Li, U. Villa, N. Duric, M.A. Anastasio, A Forward Model Incorporating Elevation-Focused Transducer Properties for 3-D Full-Waveform Inversion in Ultrasound Computed Tomography, IEEE Trans Ultrason Ferroelectr Freq Control 70 (10) (2023) 1339–1354.
[23] E.L. Bradley 3rd, J. Sacerio, The velocity of ultrasound in human blood under varying physiologic parameters, J Surg Res 12 (4) (1972) 290–297.
[24] V.M. Nahirnyak, S.W. Yoon, C.K. Holland, Acousto-mechanical and thermal properties of clotted blood, J Acoust Soc Am 119 (6) (2006) 3766–3772.
[25] L. Guasch, O. Calderón Agudo, M.X. Tang, P. Nachev, M. Warner, Full-waveform inversion imaging of the human brain, NPJ Digit Med 3 (2020) 28.
[26] P. Marty, C. Boehm, A. Fichtner, Acoustoelastic full-waveform inversion for transcranial ultrasound computed tomography, 2021.
[27] P. Marty, C. Boehm, A. Fichtner, Acoustoelastic full-waveform inversion for transcranial ultrasound computed, Proc. SPIE 11602, Medical Imaging 2021:

Ultrasonic Imaging and Tomography (15 Feb 2021) 1160211, https://doi.org/10.1117/12.2581029.

[28] J. Tong, X. Wang, J. Ren, M. Lin, J. Li, H. Sun, F. Yin, L. Liang, Y. Liu, Transcranial Ultrasound Imaging With Decomposition Descent Learning-Based Full Waveform Inversion, IEEE Trans Ultrason Ferroelectr Freq Control 69 (12) (2022) 3297–3307.

[29] G. Frija, D.H. Salama, M.G. Kawooya, B. Allen, A paradigm shift in point-of-care imaging in low-income and middle-income countries, EClinicalMedicine 62 (2023) 102114.